

# Production of $\Sigma(1385)^{\pm}$ and $\Xi(1530)^0$ measured by ALICE in pp, p–Pb and Pb–Pb collisions at the LHC

Jihye Song (for the ALICE Collaboration)

*Department of Physics, Pusan National University, Pusan, South Korea*

## Abstract

The measurement of resonances in ultra-relativistic heavy-ion collisions allows one to study the properties of the hadronic medium. Resonances with short lifetimes compared to the duration of the time span between chemical and kinetic freeze out are good candidates to probe the interplay of particle re-scattering and regeneration in the hadronic phase, which result in a modification of their measured yields. Measurements of  $\Sigma(1385)^{\pm}$  and  $\Xi(1530)^0$  have been performed with the ALICE detector in pp, p–Pb and Pb–Pb collisions at LHC energies. We report on  $p_T$ -integrated yield ratios as function of charged-particle multiplicity density,  $\langle dN_{ch}/d\eta_{lab} \rangle$ , which is used as a proxy for the size of collision system. These results complement the information derived from the measurement of other resonances such as  $K^{*}(892)^0$  and  $\phi(1020)$ . The system size dependence of the yield ratio of short-lived resonances to longer-lived particles with the same strangeness content is discussed and compared to predictions from pQCD-inspired models, statistical hadronization models and EPOS.

**Keywords:** Hadronic phase; Particle production mechanism; Resonances;  $\Sigma(1385)^{\pm}$ ;  $\Xi(1530)^0$ ;

## 1. Introduction

The hadronic resonances are valuable probes to study the properties of the hadronic medium formed in ultra-relativistic heavy-ion collisions. The yield ratios of resonances to stable hadrons provide information about the re-scattering and regeneration effects in the hadronic medium. If the effect of elastic or pseudo-elastic scattering of daughter products (re-scattering), is dominant over regeneration, the resonance yield after kinetic freeze-out will be smaller than the one originally established at the chemical freeze out. Since hadronic resonances decay due to the strong interaction with decay times of the order of the lifetime of the hadronic phase ( $\sim 10$  fm/c), the measurement of the production of a comprehensive set of particles with different lifetimes (see Table 1) can be used to study the interplay of particle re-scattering and regeneration. In order to investigate those effects, the production  $K^{*}(892)^0$  and  $\phi(1020)$  mesons has been measured in pp, p–Pb and Pb–Pb collisions [3] using the ALICE detector at the LHC. Figure 1 presents the  $K^{*0}$  and  $\phi$  to  $K^{-}$  ratios as a function of  $\langle dN_{ch}/d\eta_{lab} \rangle$ . The  $K^{*0}$  to  $K^{-}$  ratio exhibits a decreasing trend from pp to peripheral and central Pb–Pb collisions, while the  $\phi$  to  $K^{-}$  ratio is nearly flat as a function of system size. The decreasing behavior of  $K^{*0}/K^{-}$  can be interpreted as a consequence of the short lifetime of  $K^{*0}$  (see Table 1). Since the lifetime of  $\Sigma^{*}(1385)^{\pm}$  is comparable with that of the  $K^{*0}$  and the lifetime of  $\Xi^{*}(1530)^0$  is between that

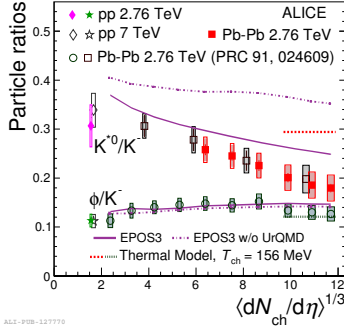


Fig. 1.  $K^0/K^-$  and  $\phi/K^-$  ratios as a function of  $\langle dN_{ch}/d\eta \rangle^{1/3}$  measured at mid-rapidity in pp collisions at  $\sqrt{s} = 2.76$  TeV and 7 TeV, and Pb-Pb collisions at  $\sqrt{s_{NN}} = 2.76$  TeV [3]. Bars represent the statistical uncertainties, empty boxes represent the total systematic uncertainties, and shaded boxes represent centrality-uncorrelated systematic uncertainties. The expectations from a thermal model calculation with chemical freeze-out temperature of 156 MeV for the most central collisions are shown. The EPOS3 predictions are also shown as a violet curves. [4]

of  $K^{*0}$  and  $\phi$ , these results may provide additional information on the relative strengths of re-scattering and regeneration.

	$c\tau$ (fm)	valence quark content	Decay modes	BR [%]
$\rho(770)^0$	1.3	$(u\bar{u} + d\bar{d})/\sqrt{2}$	$\pi^+ + \pi^-$	100
$K^*(892)^0$	4.2	$d\bar{s}$	$K^+ + \pi^-$	66.6
$\Sigma^*(1385)^+$	5.5	$uus$	$\Lambda\pi^+ \rightarrow (p\pi^-)\pi^+$	87.0
$\Lambda^*(1520)$	12.6	$uds$	$p + K^-$	22.5
$\Xi^*(1530)^0$	21.7	$uss$	$\Xi^-\pi^+ \rightarrow (\Lambda\pi^-)\pi^+ \rightarrow ((p\pi^-)\pi^-)\pi^+$	66.7
$\phi(1020)^0$	44	$s\bar{s}$	$K^+ + K^-$	48.9

Table 1. Lifetime of the measured resonances with their quark content, decay modes exploited for the measurements presented here and branching ratios (BR) [5].

## 2. Analysis and Results

Measurements of  $\Sigma^{*+}$  and  $\Xi^{*0}$  production in p–Pb collisions at  $\sqrt{s_{NN}} = 5.02$  TeV have been recently published in [6] and in addition, the  $\Xi^{*0}$  has been measured in Pb–Pb collisions at  $\sqrt{s_{NN}} = 2.76$  TeV. These baryonic resonances are studied by reconstructing their hadronic decay daughters. The intermediate decay products,  $\Lambda$  and  $\Xi^-$ , are identified through selections based on their decay topology. Combinatorial backgrounds, constructed using mixed-event technique, are subtracted from the invariant mass distributions of candidate decay-product pairs from the same event for various  $p_T$  and multiplicity event classes [6].

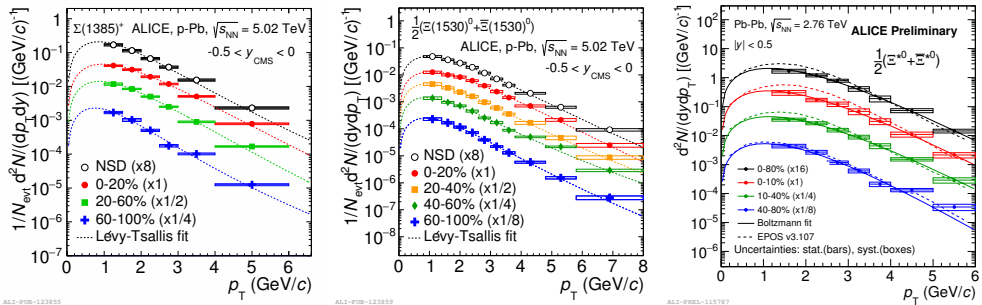


Fig. 2.  $p_T$ -spectra of  $\Sigma^{*+}$  (left) and  $\Xi^{*0}$  (middle) in p–Pb collisions at  $\sqrt{s_{NN}} = 5.02$  TeV in different V0A multiplicity event classes and the  $p_T$ -spectra of  $\Xi^{*0}$  (right) in Pb–Pb collisions at  $\sqrt{s_{NN}} = 2.76$  TeV in different centrality classes.

The  $p_T$ -spectra of  $\Sigma^{*\pm}$  and  $\Xi^{*0}$  in p-Pb collisions are measured in the range from  $1.0 < p_T < 6.0$  GeV/c and  $0.8 < p_T < 8.0$  GeV/c, and shown in the left and middle panels of Fig. 2, respectively. In Fig. 2 (right), the preliminary results for  $\Xi^{*0}$  measured in  $1.2 < p_T < 6$  GeV/c in Pb-Pb collisions are also displayed.

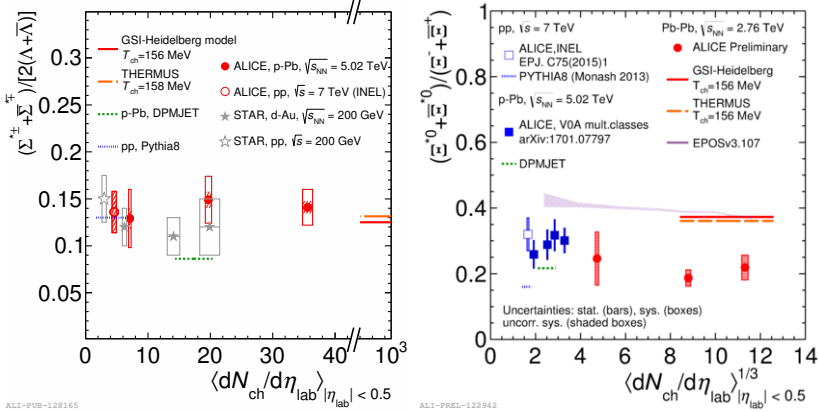


Fig. 3. (Left) Ratio of  $\Sigma^{*\pm}$  to  $\Lambda$  and (right) ratio of  $\Xi^{*0}$  to  $\Xi$  measured in pp [7, 8, 9], d-Au [10], p-Pb [11] and Pb-Pb collisions, as a function of  $\langle dN_{ch}/d\eta_{lab} \rangle$  at midrapidity. A few model predictions are also shown as lines at the appropriate abscissa.

The yield ratios of excited to stable hyperon with the same strangeness content are presented in Fig. 3 together with predictions from commonly used Monte Carlo generators, PYTHIA8 for pp and DPMJET for pPb, and thermal model predictions for Pb-Pb collisions [12, 13, 14]. The  $\Sigma^{*0}/\Lambda$  ratios are consistent with the values predicted by PYTHIA8 in pp, whereas the DPMJET prediction for p-Pb collisions underestimates the experimental data. In pp and p-Pb the ratios are higher than predicted by PYTHIA8 and DPMJET.

The constant behavior of  $\Sigma^{*0}/\Lambda$  and  $\Xi^{*0}/\Xi$  indicates that neither regeneration nor re-scattering dominate, leading to little net change of the yield of resonances in the hadronic medium. The  $\Sigma^{*0}/\Lambda$  ratios obtained by the STAR collaboration at lower energies in pp[9] and d-Au [10] collisions, also shown in Fig. 3, are compared with values at the LHC energies. In Pb-Pb,  $\Xi^{*0}/\Xi$  is lower than predicted by thermal models, despite about the five times longer lifetime with respect to  $K^{*0}$ . In addition the results are also compared with EPOSv3 with UrQMD [4], which describes a flat trend of  $\Xi^{*0}/\Xi$  as a function of  $\langle dN_{ch}/d\eta_{lab} \rangle^{1/3}$  but overestimates the value of the ratio.

These results can be compared to those shown in Fig. 4. The  $\rho(770)^0/\pi$  and  $\Lambda^*(1520)/\Lambda$  ratios are suppressed from small to large collision systems. The measurement of  $\rho^0/\pi$  is compared with EPOSv3 [4] with/without UrQMD. We have observed that the EPOSv3 prediction with UrQMD, which includes a modeling of re-scattering and regeneration in the hadronic phase, well describes the suppression trend from peripheral to central Pb-Pb collisions, while the prediction without UrQMD does not reproduce the decreasing trend. EPOSv3 with UrQMD also qualitatively describes the trends observed for not only  $\rho^0$  and  $\Lambda^*$  but also  $K^{*0}$  and  $\phi$  shown in Fig. 1. The  $\Lambda^*/\Lambda$  ratio is compared to STAR measurements in pp [9], d-Au [10] and Au-Au [9] collisions. The  $\Lambda^*/\Lambda$  results obtained in Pb-Pb  $\sqrt{s_{NN}} = 2.76$  TeV follow the trend of the results from the STAR experiment, with smaller uncertainties. All the ratios in central Pb-Pb collision are lower than the thermal model predictions. The net effect depends on the hadronic cross sections and lifetime of the resonance with respect to lifetime of the hadronic phase.

### 3. Summary

In summary, the short lifetimes of hadronic resonances enable one to study the properties of the hadronic phase in heavy-ion collisions. The baryonic resonances  $\Sigma^{*0}$  have been measured in p-Pb collisions at  $\sqrt{s_{NN}}$

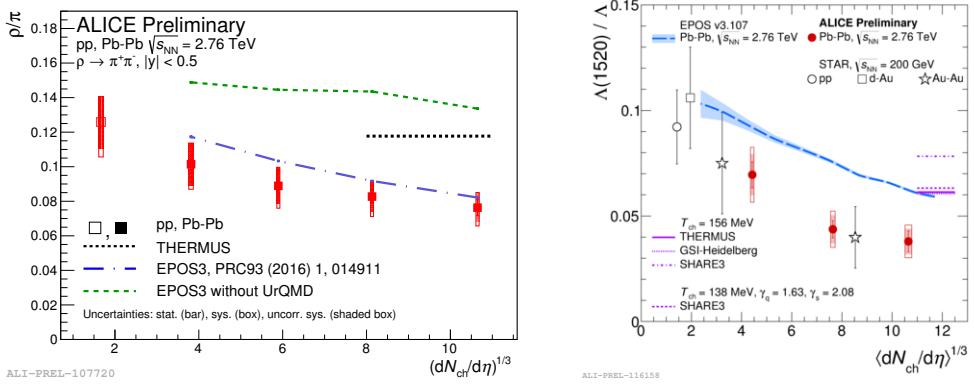


Fig. 4. (Left) Ratio of  $\rho^0/\pi$  for different system sizes in pp and Pb–Pb collisions. (right)  $\Lambda^*/\Lambda$  ratio for different system sizes compared to STAR experimental results in pp [9], d–Au [10] and Au–Au [9] collisions. Statistical uncertainties (bars) are shown as well as total systematic uncertainties (hollow boxes) and systematic uncertainties uncorrelated across  $(dN_{ch}/d\eta_{lab})^{1/3}$  (shaded boxes). All the measurements are compared with EPOS [4] and thermal model predictions [14].

= 5.02 TeV as a function of multiplicity and measurements of  $\Xi^{*0}$  are obtained in p–Pb collisions at  $\sqrt{s_{NN}} = 5.02$  TeV and in Pb–Pb collisions at  $\sqrt{s_{NN}} = 2.76$  TeV. The  $\Sigma^{*+}/\Lambda$  ratios do not vary with system size in pp and p–Pb collisions. The  $\rho^0/\pi$ ,  $K^0/K$  and  $\Lambda^*/\Lambda$  exhibit suppression from peripheral to central Pb–Pb collisions and with respect to the thermal model in central Pb–Pb collisions. This behavior is explained by the dominance of (pseudo)-elastic re-scattering of decay daughters over regeneration in the hadronic phase. Also the  $\Xi^{*0}/\Xi$  ratio in central Pb–Pb collisions shows suppression with respect to pp, p–Pb and thermal model predictions despite having a lifetime of 22 fm/c, longer than the one expected for the hadronic phase. With the present uncertainties, it cannot be concluded that the  $\Xi^{*0}/\Xi$  ratio follows a suppression pattern from peripheral to central Pb–Pb, similar to the short lived resonances. The ALICE Collaboration is currently extending these measurements to higher energies, other resonances and other collision systems. In particular, the measurements of  $\Lambda^*$  in pp and p–Pb collisions and  $\Sigma^{*+}$  in Pb–Pb are being carried out and will provide important information to constrain even further the properties of the hadronic phase.

## References

- [1] G. Torrieri and J. Rafelski 2002 *J. Phys. G* **28** 1911.
- [2] J. Rafelski, J. Letessier, and G. Torrieri 2001 *Phys. Rev. C* **64** 054907.
- [3] J. Adam, et al., ALICE Collaboration, arXiv:1702.00555
- [4] A.G. Knospe, C. Markert, K. Werner, J. Steinheimer and M. Bleicher 2016 *Phys. Rev. C* **93** 014911.
- [5] K.A. Olive, et al., Particle Data Group 2014 *Chin. Phys.* **C38** 090001.
- [6] D. Adamová, et al., ALICE Collaboration, arXiv:1701.07797
- [7] B. Abelev et al. (ALICE Collaboration) 2015 *Eur. Phys. J. C* **75** 1.
- [8] B. Abelev et al. (ALICE Collaboration) 2012 *Phys. Lett. B* **712** 309.
- [9] B. I. Abelev et al. (STAR Collaboration) 2006 *Phys. Rev. Lett.* **97** 132301.
- [10] B. I. Abelev et al. (STAR Collaboration) 2008 *Phys. Rev. C* **78** 044906.
- [11] J. Adam et al. (ALICE Collaboration) 2014 *Phys. Lett. B* **728** 25–38.
- [12] Sjöstrand, T. and Mrenna, S. and Skands, P. 2008 *Comput. Phys. Commun.* **178** 852–867.
- [13] S. Roesler, R. Engel, and J. Ranft 2000 *Conference Proceedings, MC2000, Lisbon, Portugal, October 23 – 26* 1033. arXiv:hep-ph/0012252.
- [14] S. Wheaton, J. Cleymans, and M. Hauer 2009 *Comp. Phys. Comm.* **180** 84–106.